

Electronic Supplementary Information (ESI)

Mesoporous Mn₃O₄-CoO Core-Shell Spheres Wrapped by Carbon Nanotubes: A High Performance Catalyst for the Oxygen Reduction Reaction and CO Oxidation

Junwu Xiao,^{*a} Lian Wan,^a Xue Wang,^b Qin Kuang,^b Shuang Dong,^a Fei Xiao,^a and Shuai Wang^{*a}

^aDepartment of Chemistry and Chemical Engineering, Hubei Key Laboratory of Material Chemistry and Service Failure, Key Laboratory for Large-Format Battery Materials and System, Ministry of Education, Huazhong University of Science & Technology, Wuhan, PR China

^bDepartment of Chemistry, College of Chemistry and Chemical Engineering, Xiamen University, Xiamen, 361005, PR China.

E-mail: chjwxiao@hust.edu.cn, chmsamuel@hust.edu.cn

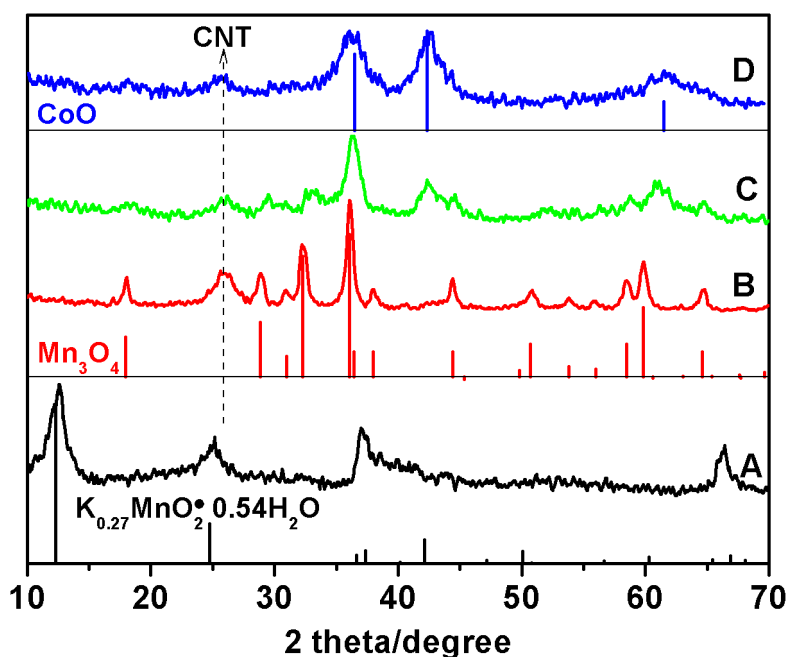


Figure SI-1. XRD patterns of the products obtained in the Step I (A), II (B), IV (C) and V (D) of Figure 1. The peak labeled by the arrow is ascribed to the diffraction peak of CNT. According to the standard XRD patterns of $K_{0.27}MnO_2 \cdot 0.54H_2O$ (JCPDS 86-0666), Mn_3O_4 (JCPDS 24-0734), and CoO (JCPDS 48-1719), it can be found that the products obtained in the Step I (A), II (B), IV (C) and V (D) correspond to the $K_{0.27}MnO_2 \cdot 0.54H_2O/CNT$, Mn_3O_4/CNT , Mn_3O_4-CoO/CNT , and CoO/CNT nanocomposites, respectively.

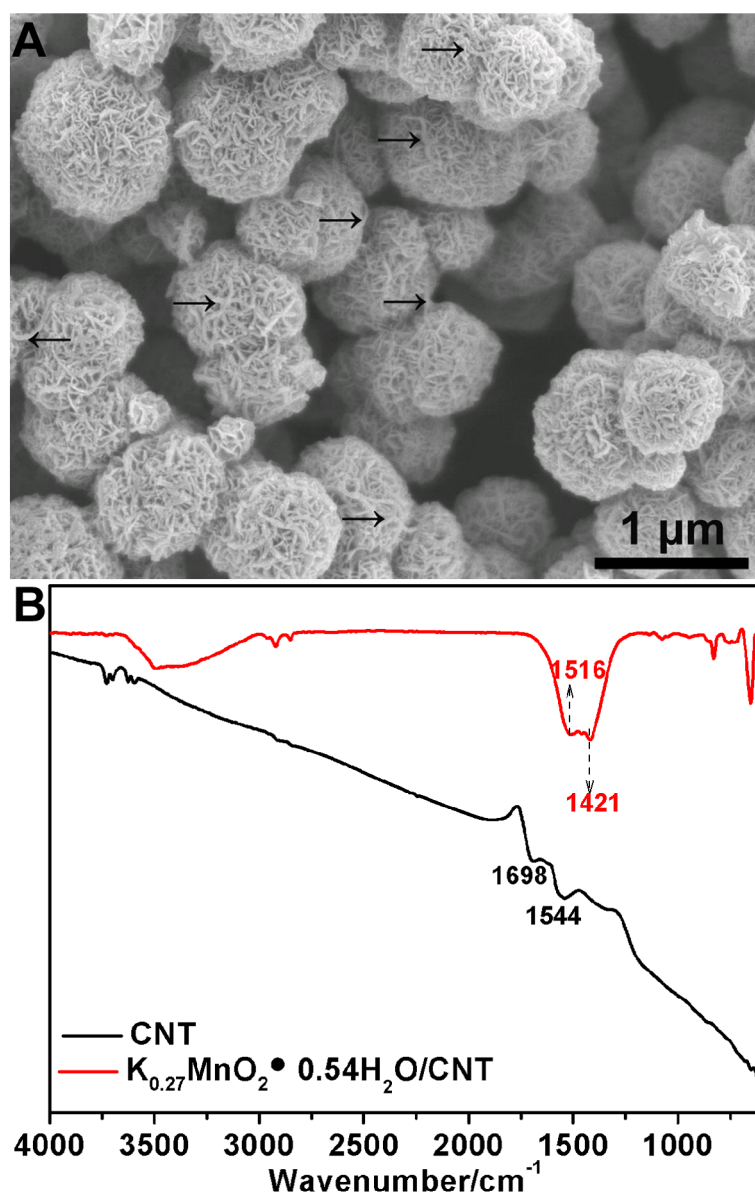


Figure SI-2. (A) SEM image of the $K_{0.27}MnO_2 \cdot 0.54H_2O$ /CNT composites (arrow: CNT), and (B) Fourier transform infrared spectra (FT-IR) of the pristine CNT and $K_{0.27}MnO_2 \cdot 0.54H_2O$ /CNT composites. As compared with that in the pristine CNT, the asymmetric and symmetrical stretching vibration of C=O in the $K_{0.27}MnO_2 \cdot 0.54H_2O$ /CNT composites shift to lower wavenumber, such as, from 1698 to 1516 cm^{-1} , and 1544 to 1421 cm^{-1} . This shift can be ascribed to the formation of COO-M (M=K, Mn) in the $K_{0.27}MnO_2 \cdot 0.54H_2O$ /CNT composites.

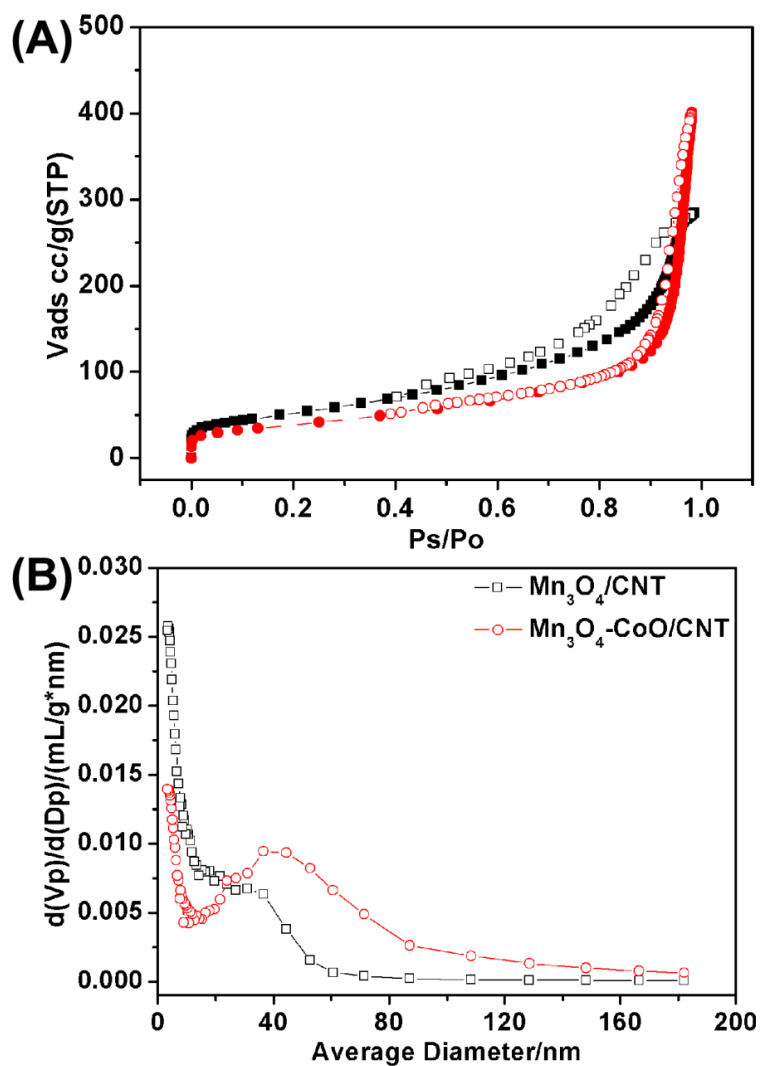


Figure SI-3. N₂ adsorption (solid)-desorption (hollow) isotherms of the Mn₃O₄/CNT (square) and Mn₃O₄-CoO/CNT (circle) nanocomposites measured at standard temperature and pressure, and (B) the corresponding BJH pore size distribution.

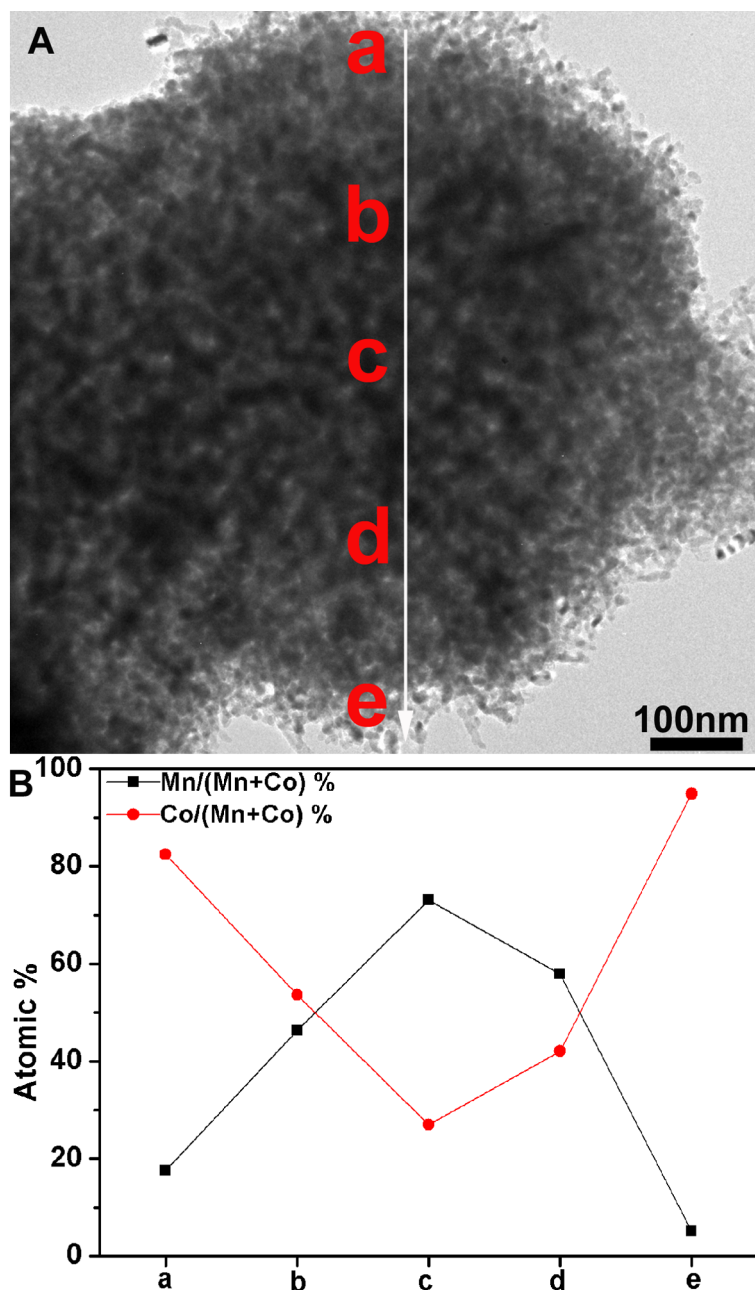


Figure SI-4. (A) TEM image of the Mn₃O₄-CoO/CNT spheres, and (B) the Mn and Co atomic percentages in the position a-e labeled in (A). We can see that Co and Mn element are dominant in the edge and center of the spheres, respectively. It indicates that the Mn₃O₄ and CoO components distribute in the core and shell, respectively, forming the Mn₃O₄-CoO core-shell spheres.

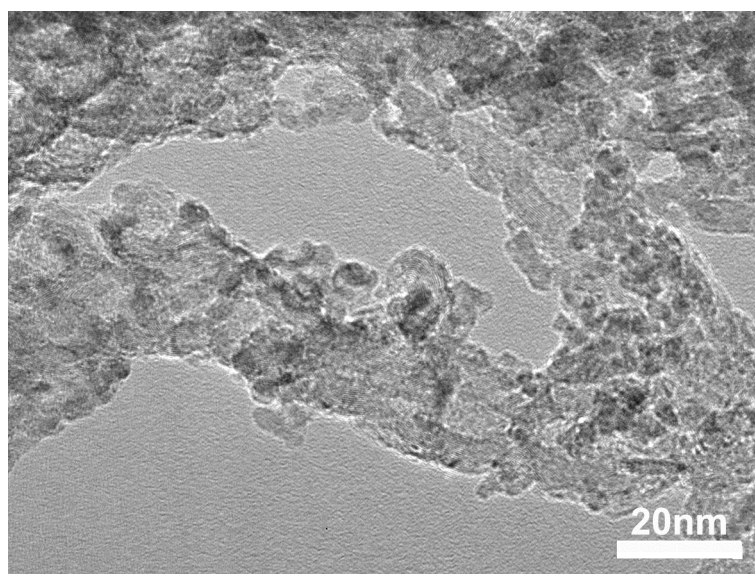


Figure SI-5. TEM images of the CoO/CNT nanocomposites.

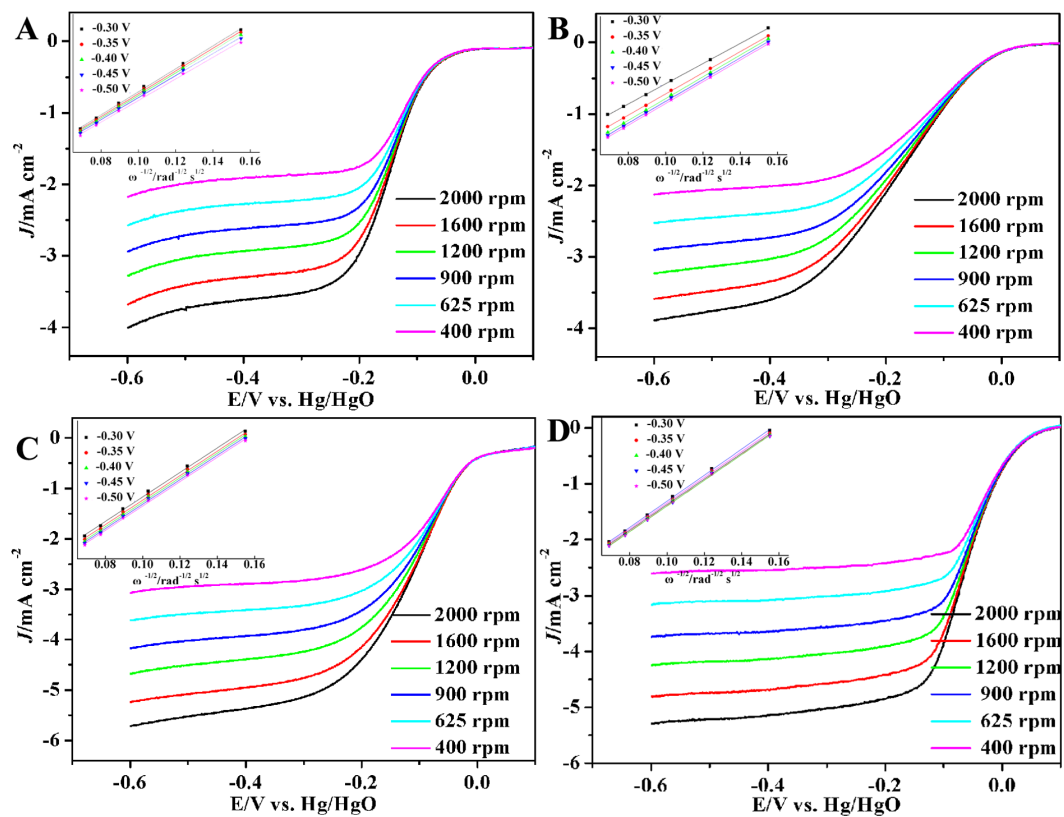


Figure SI-6. Rotating disk voltammograms at different rotation rates of (A) the $\text{Mn}_3\text{O}_4/\text{CNT}$, (B) CoO/CNT , (C) $\text{Mn}_3\text{O}_4\text{-CoO}/\text{CNT}$, and (D) the commercial Pt/C electrodes in O_2 -saturation 0.1 M KOH electrolyte. (Inset: the corresponding Koutecky-Levich plots at different electrode potentials)

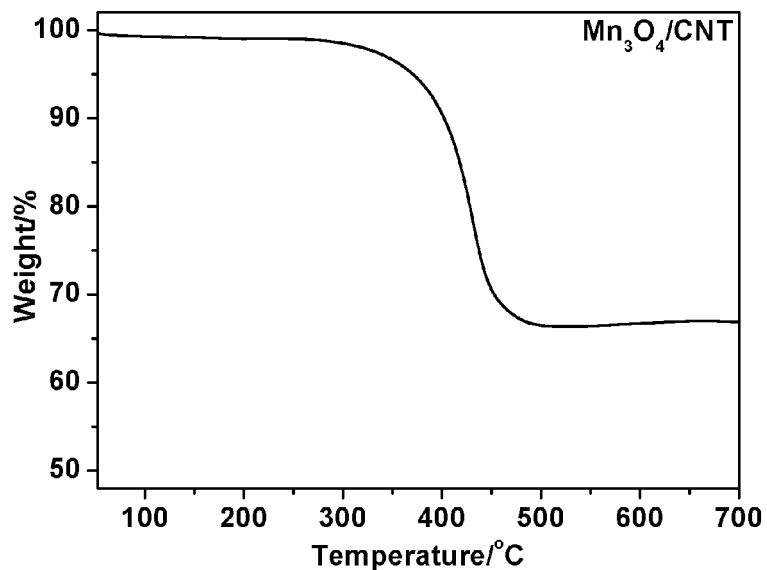


Figure SI-7. TGA result of the Mn₃O₄/CNT composites, which was performed from 50 to 700 °C at a heating rate of 5 °C min⁻¹ under an air flow of 25 mL min⁻¹. There is no weight loss at < 250 °C for the Mn₃O₄/CNT composites, indicating that CNT are very stable in this temperature range.